Contrasting biogeochemical processes revealed by stable isotopes of H2O, N, C and S in shallow aquifers underlying agricultural lowlands

Article *in* Science of The Total Environment · July 2019

DOI: 10.1016/j.scitotenv.2019.07.238

4 authors:

Nicolò Colombani
Università Politecnica delle Marche

Micòl Mastrocicco
Università degli Studi della Campania "Luigi Vanvitelli

Giuseppe Castaldelli
University of Ferrara

Ramón Aravena
University of Waterloo

Contrasting biogeochemical processes revealed by stable isotopes of H_2O, N, C and S in shallow aquifers underlying agricultural lowlands

Nicolò Colombani[1], Micol Mastrocicco[2#], Giuseppe Castaldelli[3], Ramon Aravena[4]

[1]SIMAU - Department of Materials, Environmental Sciences and Urban Planning, Polytechnic University of Marche, Via Brecce Bianche 12, 60131 Ancona, Italy

[2]DiSTABiF - Department of Environmental, Biological and Pharmaceutical Sciences and Technologies, Campania University "Luigi Vanvitelli", Via Vivaldi 43, 81100 Caserta, Italy

[3]SVeB - Department of Life Sciences and Biotechnology, University of Ferrara, Via L. Borsari 46, 44121 Ferrara, Italy

[4]Department of Earth and Environmental Sciences, University of Waterloo, 200 University Avenue West, Waterloo, ON N2L 3G1, Canada

[#]Corresponding author: Prof. Micòl Mastrocicco (micol.mastrocicco@unicampania.it)

Abstract

Lowland coastal areas as the Po Delta (Italy) are often intensively cultivated and affected by nitrogen imbalance due to fertilizers leaching to groundwater and export via run-off. To address this issue several agricultural best practices have been proposed, like limiting the amount of fertilizers and increasing soil organic matter content. In this study, groundwater samples were analysed for major ions and stable isotopes of H_2O, C, N and S using multi-level sampler (MLS) from two contrasting depositional environments, one representative of alluvial plain (AP) and the other representative of a reclaimed coastal plain (RCP). In each site, controlled plots with different agriculture practice including fertilizers and tillage and compost amendment and no tillage were considered in the study. Tracer test results highlight that recharge water infiltrated at the start of the controlled study has not yet reached the saturated zone, thus current groundwater concentrations are representative of former agricultural practices. Stable isotopes show a clear distinction between different sources of nitrogen in both sites, from synthetic fertilizers to sedimentary nitrogen pool and atmospheric input. The main source of sulphate in groundwater are pyrite and fertilizers. Denitrification, sulphate reduction and methanogenesis were involved in the C, N and S cycle in the RCP site characterized by low hydraulic conductivity sediments and high SOM. These processes were not relevant in the AP site characterized by oxic condition and low SOM, but some evidence of denitrification was found in one of the AP sites. High resolution monitoring was a key tool to identify the different redox zones responsible for N, C and S cycling in these aquifers. This study shows that a clear understanding of transit times in the vadose zone is a key prerequisite to evaluate the effect of controlled agriculture practice on the quality of shallow groundwater.

Keywords

Recharge, transit time, denitrification, shallow aquifer, fertilizers leaching, redox zones.

1. Introduction

The impact of intensive agriculture on the underlying aquifers in coastal lowlands has been the target of many recent studies focusing on nitrate (NO_3^-) concentrations in groundwater (Oenema et al., 2005; Wu and Sun, 2016; Paradis et al., 2018). The role of denitrification, the microbial-mediated reduction of NO_3^- which is often connected with reduced environments rich in sedimentary organic matter (SOM) (Rivett et al., 2008; Taylor and Townsend, 2010) and pyrite (Zhang et al., 2012), is a key process that has to be evaluated in NO_3^--related studies in groundwater. Pyrite oxidation in the unsaturated zone (by oxygen) and in the saturated zone (involved in denitrification) leads to sulphate (SO_4^{2-}) release and often to trace metal mobilization, in turn impacting the local and regional water quality (Zhang et al., 2013).

The evaluation of geochemical processes at sites impacted by agriculture activities often involve the use of a combination of hydrogeological, chemical and isotopes tools (Böhlke and Denver, 1995; Hosono et al., 2013). Water stable isotopes ($\delta^{18}O$ and $\delta\ ^{2}H$) usually provide information about the role of the different sources of water that can be involved in recharge processes in agricultural settings, including local precipitation and recirculation of water from irrigated fields (Criss and Davisson, 1996; Fernández et al., 2017). Furthermore, the stable isotopes of NO_3^- and SO_4^{2-} (^{15}N and ^{18}O, ^{34}S and ^{18}O, respectively) are often used to evaluate sources and processes that affect these compounds in groundwater (Aravena and Robertson, 1998; Kaown et al., 2009; Pauwels et al., 2010). The use of isotopic tools in combination with a detailed hydrogeological and chemical characterization provides information to develop a robust conceptual model in terms of origin and transformation processes affecting major dissolved species in agriculture settings (Biddau et al., 2019; Puig et al., 2017).

A key component acting on NO_3^- attenuation in groundwater is the nature of geological materials forming the aquifer (Böhlke, 2002; Mastrocicco et al., 2011; Clague et al., 2019). Low hydraulic conductivity sediments play an important role in the attenuation of N compounds in groundwater (Yan et al., 2016) and can substantially increase the transit time in the vadose zone (Green et al., 2018). The present study aims to contribute to the knowledge of shallow geological heterogeneities

importance in driving geochemical processes affecting dissolved species associated to agricultural activities in lowland environments under different agriculture practices. The study provides a clear framework to monitor N, S and C cycling in shallow groundwater, starting from the hydrogeological characterization, to residence times and the geochemical processes, by using high vertical resolution data.

2. Material and Methods

2.1. Study sites

The Po river Plain (Northern Italy) has been intensively cultivated since the last century because of its flat topography and the large surface water availability. This region is largely threatened by agrochemical leaching, especially nutrients like NO_3^- (Martinelli et al., 2018), so that the most important hydrogeological and microbial processes affecting NO_3^- fate and transport in the local aquifers have been extensively studied (Castaldelli et al., 2013; Caschetto et al., 2017; Mastrocicco et al., 2017). The two field sites (1 ha each) selected for this study are located in the Po Delta (Ferrara Province), at an altitude ranging from 5 to -3 m above sea level (m.a.s.l.) and are instrumented with Multi-level samplers (MLS) for water samples collection (chemical and isotopic analysis) and hydrogeological measurements (Figure 1). The first site, named alluvial plain (AP), pertains to a freshwater paleo-river environment, while the second site, named reclaimed coastal plain (RCP), pertains to a reclaimed brackish swamp environment (Figure 1). MLSs consist of PVC nested mini-wells with an internal diameter of 2 cm screened in the last 20 cm with a 50 μm Nitex mesh. The MLSs installed in plots with standard use of fertilizers and tillage were named RCP_{ST} and AP_{ST}, while MLSs installed in plots with the experimental set up, where compost was incorporated within the top 15 cm of soil and no-tillage was applied, were named RCP_{EXP} and AP_{EXP} (Figure 1).

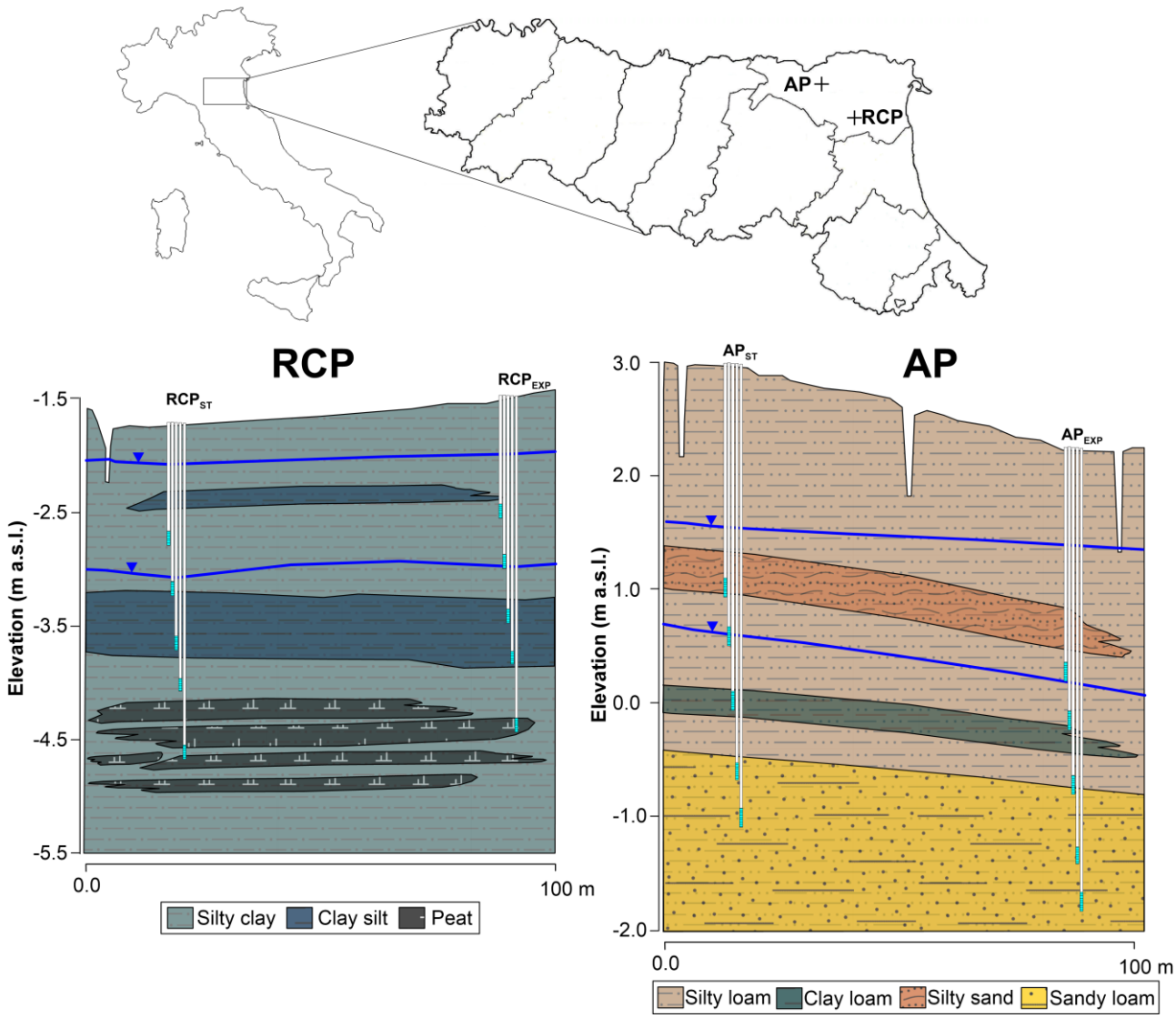

Figure 1: The upper panel shows the location of the two field sites and the lower panel shows geological profiles and the MLSs' depth design; the main geological lenses and the average water table elevation in summer (lower blue lines) and winter (upper blue lines) are also shown.

The soil in AP is a Hypocalcic Haplic Calcisol, moderately alkaline, with the upper horizons characterized by silty clay loamy texture and the lower horizons with calcareous silty loamy textures. The soil in RCP is a Calcaric Gleyic Cambisol, moderately alkaline, with silty clay or clay loamy textures and peaty lenses at 2.0-2.5 m below ground level (m.b.g.l.). These soils were selected since they are representative of the most common environments of the Po river lowland.

Both soils are cultivated with a rotation of wheat and maize with a N fertilization based on NPK mineral fertilizers, NH_4NO_3 and synthetic urea with a total average rate of 170 kg N/ha/y. This area has been declared vulnerable to NO_3^- by the Italian environmental authority following the enactment of the European Water Framework Directive (2000/60/CE). The two sites are investigated as part of a research project, supported by the Rural Development Programme of the Emilia-Romagna Region (PSR 2014-2020), aiming to reduce the environmental impact of agricultural practices by comparing the use of compost and no-tillage techniques versus the classical fertilization and tillage techniques.

2.2. Sampling and analytical methods

Piezometric heads in each MLS port were measured monthly since 2016 and will be monitored until the end of 2019. Slug tests were performed in all piezometers to estimate the hydraulic conductivity (*K*) using a pneumatic initiation system to instantaneously lower the static groundwater level of approximately 0.5 m. The slug test data were analysed using the Bouwer and Rice (1976) method.

A Bromide (Br^-) tracer test was carried out in each plot. An area of 0.1 m^2 was irrigated with 1 L deionized water containing 1000 mg/L of Br^- at the beginning of the experiment (30/10/2016). After 18 months (30/04/2018), an auger corer was used to collect soil samples every 10 cm in the same locations where the tracer tests were performed, to monitor Br^- migration in the unsaturated zone. Soil cores were extracted with deionized water with a liquid solid ratio of 10:1 and the solution was analysed using a Br^- ion selective electrode (NexSens, USA). Soil water content and dry bulk density were measured gravimetrically. The detection limit for Br^- in soil cores was 2.0 mg/dm^3 of soil. The MLSs were sampled in March 2018 to evaluate the hydrogeochemical parameters. The standard well sampling procedure was followed when possible, removing a water volume equivalent to 3 times the standing water column. However, some monitoring wells in RCP recharged so slowly that wells had to be purged the day before sampling, and removal of more than one standing water column was unfeasible. A low flow sampling method was employed to

minimise cross contamination from nearby layers, using an inertial pump with the flow rate limited to 100-150 ml/min. A flow cell equipped with electric conductivity (EC), dissolved oxygen, pH and oxygen reduction potential (ORP) portable HANNA Instr. Probes was used. Water samples were taken once parameters had been stable for at least 5 min. All samples were stored in a fridge at 4°C, kept in a dark environment and immediately transported to the laboratory for proper conservation prior to be analysed.

Major anions (along with acetate and formate) were analysed using an isocratic dual pump ion chromatography ICS-1000 Dionex. Methane (CH_4) in groundwater samples was analysed by MIMS-Membrane Inlet Mass Spectrometry (Bay Instruments, USA), consisting in a PrismaPlus quadrupole mass spectrometer with an inline furnace operating at 600°C to allow for O_2 removal. CH_4 concentrations were quantified by the ion current detected at m/z ratio of 15. Samples for CH_4 determination were collected by overflowing at least 3 times a 12-ml gas-tight glass vials (Exetainer®, Labco, High Wycombe, UK) and preserved by adding 100 µL of 7M $ZnCl_2$ solution. Dissolved organic carbon (DOC) and dissolved inorganic carbon (DIC) were measured with a Carbon Analyzer Shimadzu TOC-V-CSM in a 5 ml sub-aliquot of groundwater sample. Hydrogen sulphide (H_2S) and NH_4^+ were measured spectrophotometrically on a double beam Jasco V-550 spectrophotometer using HACH LCK cuvette kit tests in a 5 ml sub-aliquot of groundwater sample.

Stable isotopes composition was determined at the Isotope Laboratory of the University of Waterloo, Canada. $\delta^{18}O$ and $\delta^{2}H$ analyses in water samples were carried out using a CRDS Los Gatos LWIA 24-d isotopic analyser; the analytical error was ±0.1‰ for $\delta^{18}O$ and ±1‰ for $\delta^{2}H$.

For $\delta^{15}N_{NO3}$ and $\delta^{18}O_{NO3}$ analyses, samples (50 ml) were run after conversion of NO_3^- to nitrous oxide (N_2O) by chemical denitrification (Ryabenko et al., 2009). Samples containing 2 µg of NO_3^- as N were freeze dried and then re-dissolved in a 3 mL sodium-chloride/imidazole solution. Following re-dissolution, activated cadmium was added to reduce NO_3^- to nitrite (NO_2^-) over a 24-hour period. Samples were then syringe filtered into helium-filled 20 mL serum vials; a buffer solution (acetic acid and sodium azide) was added to convert NO_2^- to N_2O. After allowing the

reaction to proceed to completion, a sodium hydroxide solution was added to quench the reaction. N_2O samples were analysed for $\delta^{15}N_{NO3}$ and $\delta^{18}O_{NO3}$ by injection of 10-15 nmol of N_2O into a GV Trace Gas pre=concentrator system, attached to a GV Isoprime mass spectrometer. The Trace Gas system further purified the sample and chromatographically separated N_2O from any remaining trace of CO_2. Replicate samples and standards are typically within ±0.5‰ for both $\delta^{15}N_{NO3}$ and $\delta^{18}O_{NO3}$.

For $\delta^{15}N_{NH4}$, 100 mL samples were collected, adjusted to pH 4.5-5 with 20% H_2SO_4 and frozen until analysed. Based on sample concentration, a target amount of approximately 20-50 µg of N was used for the analysis. The appropriate amount of sample was placed in a 60ml jar with 4M KCl solution and a phenolphthalein indicator was added. Sample was treated with NaOH until the solution turned bright pink. A buffer solution of Sodium TetraBorate was added and a Teflon packet containing an acidified quartz disc was added and sealed in the jar. After 10 days, NH_4^+ in the sample should have volatilized into ammonia and absorbed onto the acidified quartz disc, as Teflon is permeable to gas. The disc was removed, frozen and freeze-dried to assure no moisture remain. The disc was then folded into a tin cup and combusted on a Delta Finnigan Elemental analyser coupled with an Isotope Ratio Mass Spectrometer (IRMS). The precision associated with $\delta^{15}N_{NH4}$ analyses is generally better than ±0.2‰.

For SO_4^{2-} isotope analyses ($\delta^{34}S_{SO4}$ and $\delta^{18}O_{SO4}$), 1L samples were collected and stored at room temperature. Based on sample concentration, a target amount in the range of 20-50 µg of S was used for the analysis (Mayer and Krouse, 2004). The dissolved SO_4^{2-} was precipitated as $BaSO_4$ by adding $BaCl_2$-$2H_2O$, after acidifying the sample with HCl and boiling it to avoid interference by bicarbonates. $\delta^{34}S_{SO4}$ was determined by a Carlo Erba Elemental Analyser (EA) coupled in continuous flow to a Finnigan Delta IRMS, while analyses for $\delta^{18}O_{SO4}$ were run using an Isochrom IRMS Micromass coupled to the EA with a high temperature furnace. Reproducibility of the samples calculated from standards interspersed in the batches was 0.2% for $\delta^{34}S_{SO4}$ and $\delta^{18}O_{SO4}$.

For $^{13}C_{DIC}$, water samples (50 ml) were injected in capped vacutainer 12 mL vials and few drops of 85% phosphoric acid were added. The vials were then shaken vigorously for 10 minutes and the analyses were carried out using an Agilent 6890 coupled to an Isochrom (Micromass UK) continuous flow IRMS. The precision associated with $\delta^{13}C_{DIC}$ analyses is <±0.2‰. All results are reported in δ (‰) values relative to international standards: Air for $\delta^{15}N_{NO3}$ and $\delta^{15}N_{NH4}$; Vienna Canyon del Diablo Triolite (VCDT) for $\delta^{34}S_{SO4}$; Vienna Pee Dee Belemnite (VPDB) for $\delta^{13}C_{DIC}$; Vienna Standard Mean Ocean Water (VSMOW) for $\delta^{18}O_{H2O}$ and $\delta^{2}H_{H20}$, and $\delta^{18}O_{NO3}$ and $\delta^{18}O_{SO4}$. All analytical results discussed in this paper are reported in the Supplementary Information.

3. Results and discussion

3.1. Hydrogeological information

The water table at both sites is affected by seasonal fluctuation due to recharge events occurring in winter and spring, while a marked drawdown is detected in summer (Figure 1, lower panels). The latter is due to evapotranspiration processes that are quite pronounced in this area during the crop growing season (i.e. from April to September), since the water table is close to the ground surface and the soils are characterized by an elevated capillary rise (Colombani et al., 2016). Both sites host an unconfined aquifer superimposed to a confined aquifer. They are separated by a relatively thick and continuous clay and silt lens located at -3.5 m a.s.l. in RCP, and by a silty-clay lens located at 0.0 m a.s.l. in AP (Table 1). The degree of confinement is higher in RCP since the low hydraulic conductivity lenses are thicker than in AP, where the low hydraulic conductivity lenses are also thinning toward the AP_{EXP} plot, increasing the connectivity of the lower sandy aquifer with the upper soil horizons (Figure 1).

Table 1. *K* values observed in the MLSs of the two sites at different depths, for both the standard and experimental plots.

Piezometer's depth (m b.g.l.)	RCP_{ST} (m/s)	RCP_{EXP} (m/s)	AP_{ST} (m/s)	AP_{EXP} (m/s)
-1.0 at RCP; -2.0 at AP	$8.9x10^{-7}$	$5.3x10^{-7}$	$1.3x10^{-5}$	$7.7x10^{-6}$
-1.5 at RCP; -2.5 at AP	$8.1x10^{-7}$	$3.3x10^{-7}$	$8.7x10^{-6}$	$8.1x10^{-6}$
-2.0 at RCP; -3.0 at AP	$1.2x10^{-7}$	$3.0x10^{-7}$	$2.2x10^{-7}$	$6.2x10^{-7}$
-2.5 at RCP; -3.5 at AP	$4.2x10^{-7}$	$1.1x10^{-7}$	$1.1x10^{-5}$	$4.2x10^{-5}$
-3.0 at RCP; -4.0 at AP	$2.1x10^{-6}$	$4.3x10^{-6}$	$3.5x10^{-5}$	$5.0x10^{-5}$

3.2 EC and ORP profiles

In RCP (Figure 2, upper panels), EC increases with depth reaching values up to 7 mS/cm. This is due to brackish paleo-marshes, which are quite widespread in the shallow coastal aquifers of the Po river lowland (Greggio et al., 2018). ORP shows a decreasing trend with depth reaching values as low as -300 mV, typical of very reduced redox conditions triggered by the concurrence of low hydraulic conductivity sediments with abundance of SOM within the peat lenses. In AP (Figure 2, lower panels), EC is lower than in RCP, with maximum values up to 2 mS/cm, reached within the clay loam lenses. ORP is always positive, suggesting oxic and sub-oxic redox conditions, due to a general lack of SOM and readily available substrates like low molecular weight organic acids (Mastrocicco et al., 2017).

The pH is circumneutral in RCP with an average value of 6.8 and slightly basic in AP with an average value of 7.8 (See Supplementary Information). These values are consistent with calcite buffered systems and the slightly acidic conditions of RCP are due to the excess of SOM.

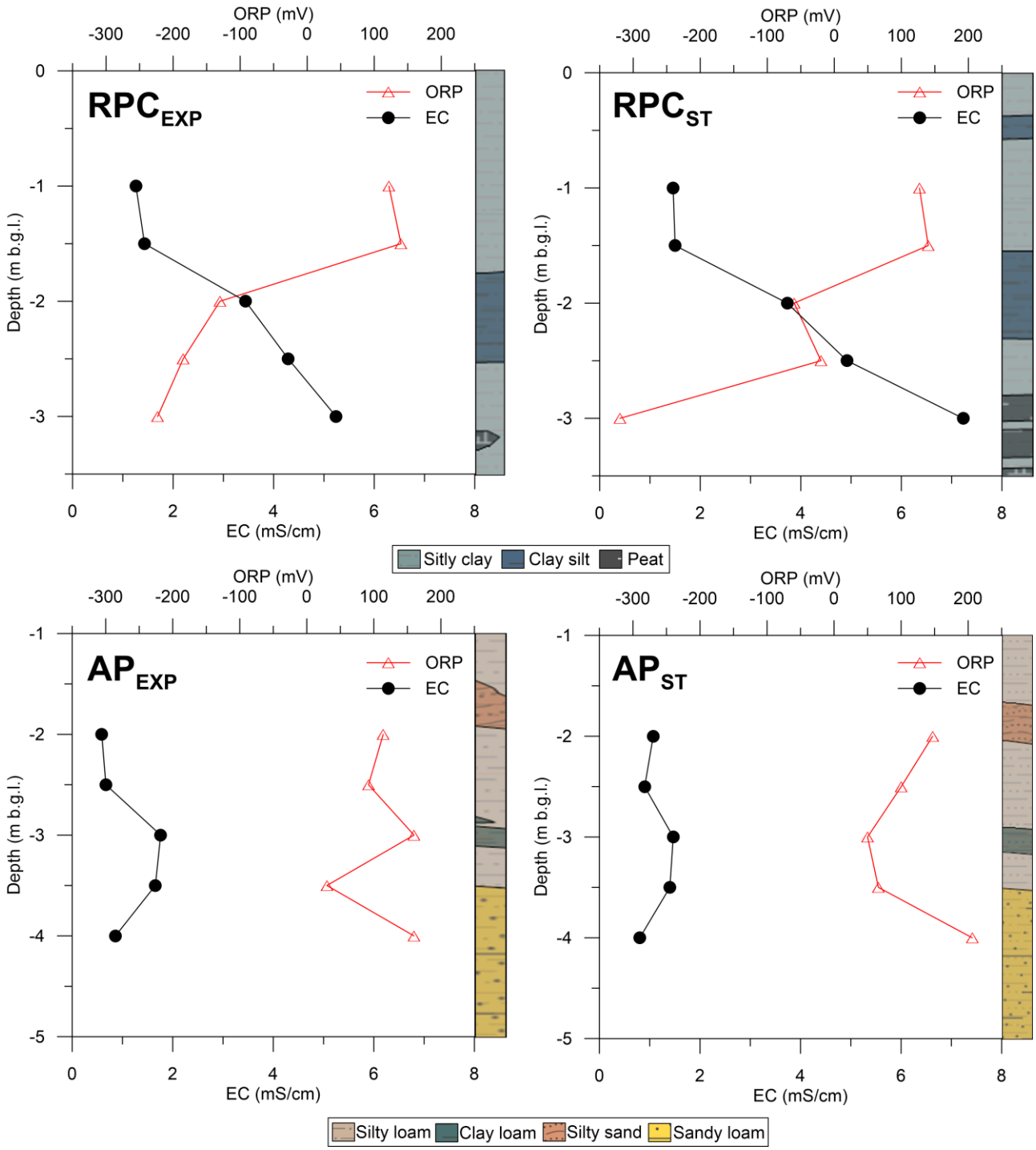

Figure 2. Groundwater ORP and EC profiles recorded in the MLSs at the RCP site (upper panels) and AP site (lower panels).

3.2. δ^2H-H_2O and δ^{18}O-H_2O groundwater characterization

The stable isotope data show a relatively large range of isotope composition that varies from -6‰ to -10‰ for δ^{18}O-H_2O and from -40‰ to -70‰ for δ^2H-H_2O (Figure 3, left plot). The most

isotopically depleted water pertains to AP while the most enriched one pertains to RCP and given that the altitude gradient is negligible between the two sites, the isotopic differences must be related to a different origin of recharge waters and/or to processes that have affected these waters. This observation is further explored by comparing the isotope data collected at both sites versus the Northern Italian Meteoric Water Line (NIMWL), recently revisited by Giustini et al. (2016). The $\delta^{18}O$-H_2O of local recharge in the study sites should be around -7‰. Then, the most isotopically depleted groundwater at RCP represents water of different origin, probably recirculating water from the irrigation canals directly diverted from the Po River. Some groundwater samples at RCP show a small contribution from recirculating waters and some show a trend diverging from the NIMWL toward more enriched isotopes values. The latter is a typical pattern related to evaporation (Horita et al., 2008) and/or to the influence of residual seawater preserved in the low hydraulic conductivity sediments.

δ^2H-H_2O values against Cl^- concentrations (Figure 3, right plot), supports the role of residual seawater, since the samples characterized by concentration of Cl^- higher than 1000 mg/L tend to a common end-member, indicating mixing with brackish waters typical of back barrier and wetland environments present in this reclaimed area until a few centuries ago (Curzi et al., 2006).

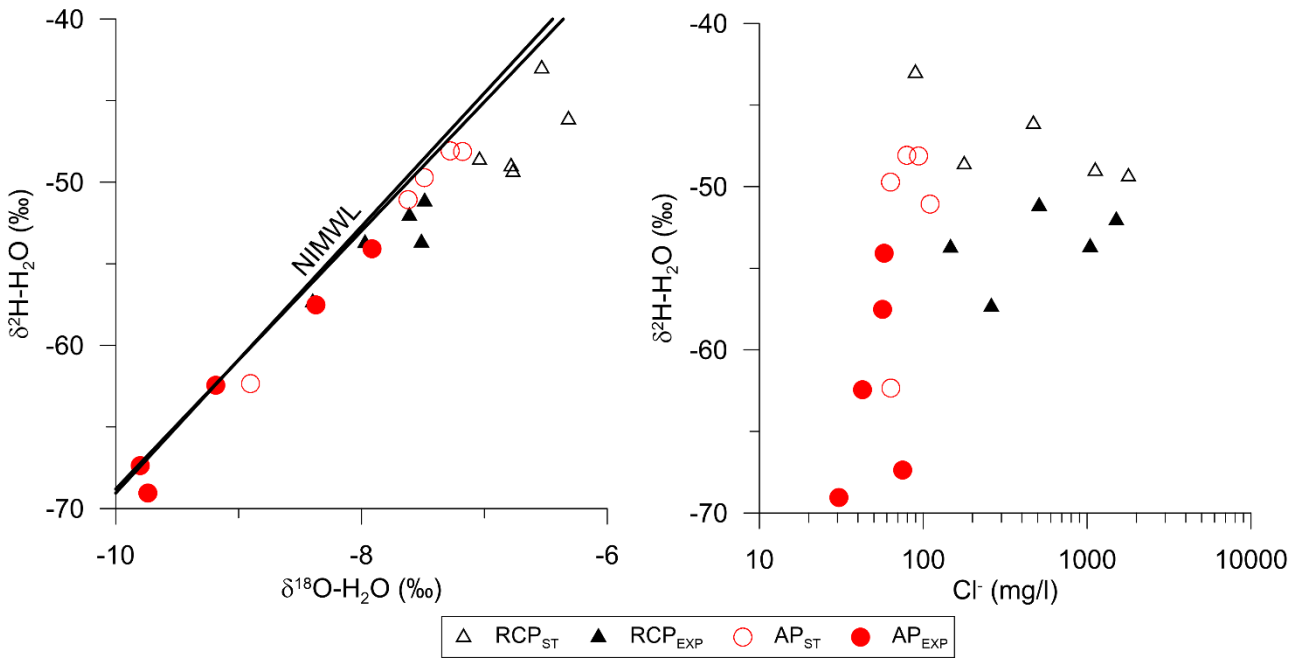

Figure 3. Left plot: water stable isotopes composition at RCP and AP, the upper and lower estimates for the Northern Italian Mean Water Line (NIMWL) are also plotted for comparison (Giustini et al., 2016). Right plot: relationship between Cl^- concentrations and δ^2H-H_2O at RCP and AP.

The δ^2H-H_2O and $\delta^{18}O$-H_2O depth profiles provide additional information about the water cycle in these shallow aquifers. First, these data clearly show large isotopic differences are observed among the two sites and among the standard and experimental plots within each site (Figure 4). Despite the two sets of MLSs are in the same cultivated field, just a few meters apart from each other, the RCP_{EXP} profile shows the influence of the input of a more isotopic depleted recharge water compared to the RCP_{ST} isotope profile, especially in the shallow MLS ports. This pattern leads to hypothesise that groundwater recharge is highly spatially variable due to local heterogeneities that can enhance or limit infiltration. A distinct isotopic pattern is observed in the depth profiles of AP_{EXP} compared to AP_{ST} ones. The shallow MLS ports in AP_{EXP} show the influence of the recirculating water probably associated to irrigation from nearby ditches (connected to the Po River), while the deeper MLS ports tend toward more enriched isotopic values associated to the

underlying aquifer. For AP_{ST}, the shallow MLS ports reflect the input of recharge by local precipitation, followed by a trend toward the isotopic composition of the underlying aquifer. These different patterns show the complexity of the water cycle at the study sites. The contribution of the irrigation water could be associated to leakage from the irrigation ditches, that could explain the variability of both δ^2H-H_2O and $\delta^{18}O$-H_2O. Due to the low hydraulic conductivity of the sediments in both sites, it can be postulated that the residence time in these aquitard-aquifer systems should be quite long. For this reason, the observed isotopic signatures are representative of the long-term processes that have affected these intensively cultivated agricultural landscapes in the last decades rather than the actual land use. This issue will be further debated in the next section where a Br^- tracer test experiment will be discussed.

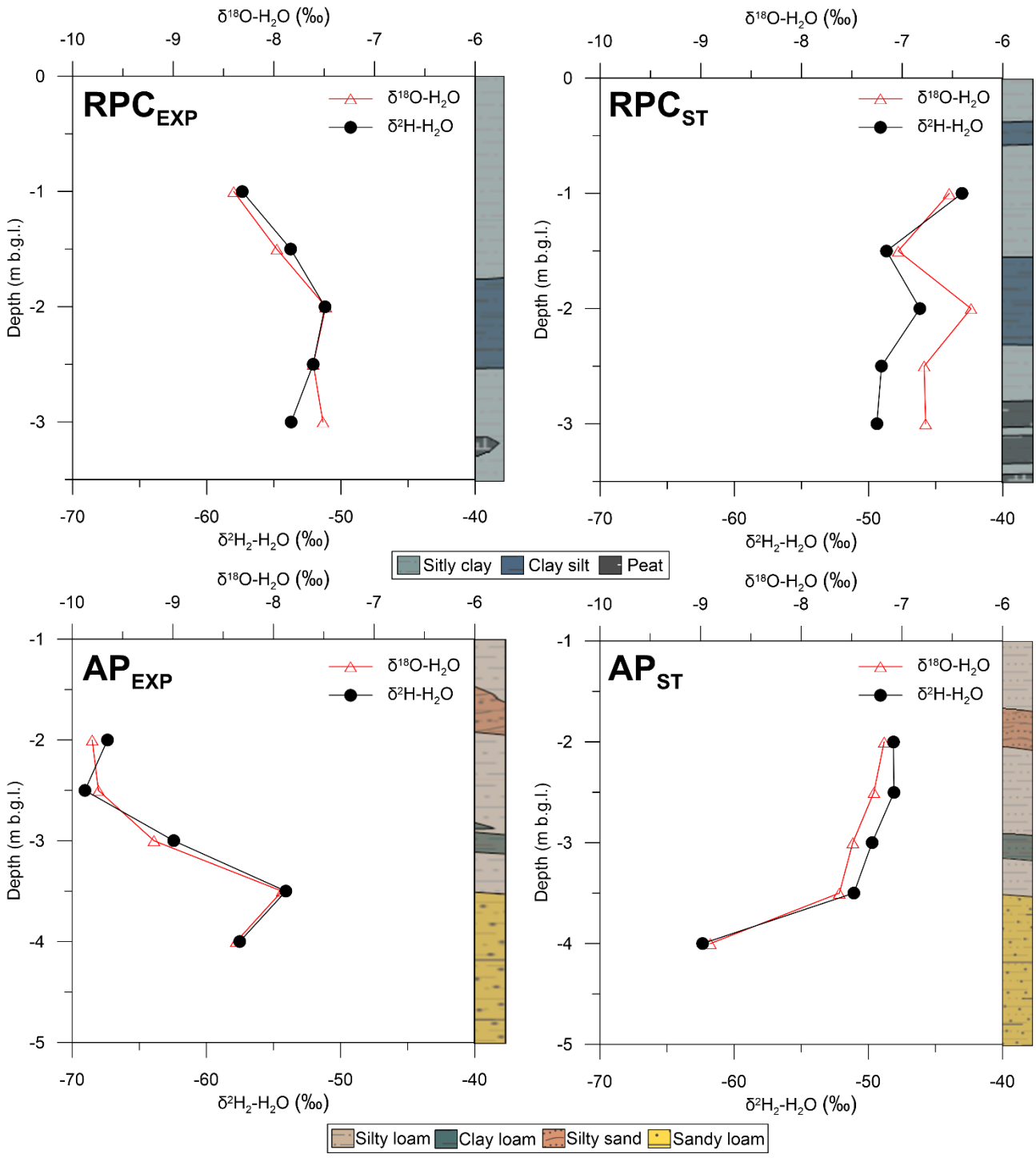

Figure 4. δ^2H-H_2O and δ^{18}O-H_2O groundwater depth profiles in the standard and experimental plots of the two field sites. Error bars are not plotted since the symbols' size is larger than the error bars.

3.3. Br^- tracer tests results

Figure 5 shows the results of the natural gradient tracer test started at the beginning of the project.

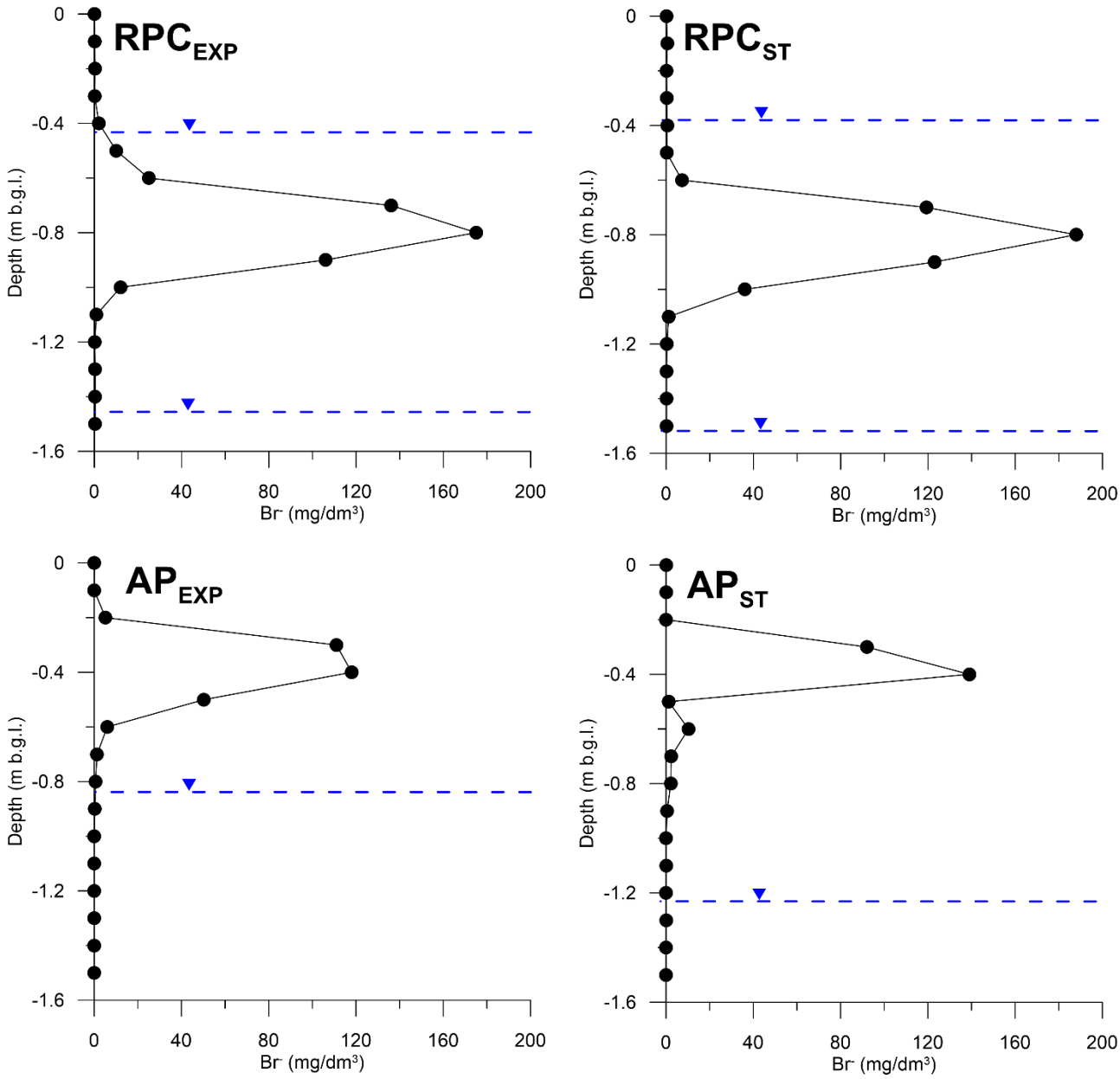

Figure 5. Br^- soil depth profiles in RCP and AP, collected in April 2018 within the tracer test areas. The blue lines represent the water table maximum and minimum depths at the RCP site and a water table maximum at the AP site.

The Br^- concentration was below the detection limit in cores collected down to -1.5 m b.g.l. in both AP and RCP before the tracer test. It can be noticed that the centre of tracer's mass has been found at -0.8 m b.g.l. in both RCP plots, while in AP it has been found at -0.4 m b.g.l. This is not surprising, since RCP has a shallower water table than AP (see the blue lines in Figure 5). Thus, the

water table reached the Br^- centre of mass during the recharge periods and transported it downward when dropping down in the summer periods. On the other hand, in AP the water table is always lower than -0.8 m b.g.l. and vertical solute transport in the vadose zone is much slower than in saturated conditions. Thus, given that Br^- profiles were obtained after 18 months, the vadose zone residence time in AP_{EXP} should be approximately 3 years, while in AP_{ST} should be approximately 4.5 years since the water table is lower than in AP_{EXP}. While, in both RCP_{EXP} and RCP_{ST} the vadose zone residence time should be approximately 1.5 years or less given that the water table is on average at -1 m b.g.l..

The most important information gained by this tracer test is that the recharge waters infiltrated after the initiation of the controlled agricultural practice experiment (PSR research project started in October 2016, see section 2.1) had not reached the sampling MLS ports at the time the chemical and isotope dataset was obtained (March 2018). Thus, the groundwater samples collected from the MLSs can be considered representative of waters infiltrated before the beginning of the project, resembling the typical fertilization practices and tillage techniques in all plots. This is extremely important for the development of a robust and correct conceptual model, since all the chemical and isotopic variability found in this study cannot be related to the actual agricultural practices but are related to the previous ones, that were similar at RCP and AP.

3.4. Nitrogen cycling

3.4.1 Reactive nitrogen concentration patterns

The vertical profiles of NO_3^- and NH_4^+ concentration for both sites are presented in Figure 6. The NH_4^+ concentrations increase with depth at RCP_{EXP} and RCP_{ST}, from 8.1 and 1.1 mg/L in the shallow MLS ports to 15.3 and 23.3 mg/L in the deep MLS ports, respectively. An opposite trend is observed for NO_3^-, which decreases from 34.5 and 20.7 mg/L in the shallow MLS ports to 2.0 and 0.2 mg/L in the deep MLS ports. The presence of NH_4^+ and NO_3^- in the shallow MLS ports indicate oxidizing conditions and probably partial conversion of NH_4^+ to NO_3^- in the unsaturated zone. The

high NH_4^+ concentration observed in the deepest part of the profiles is an indication of NH_4^+ production associated to the presence of peaty lenses that, in combination with the low hydraulic conductivity of the sediments, trigger SOM degradation and mineralization of organic N into NH_4^+. This behaviour is quite common in the study area (Mastrocicco et al., 2013; Caschetto et al., 2017) and in other alluvial plains and deltas around the world (Griffioen et al., 2013; Wang et al., 2013). The NO_3^- concentration pattern indicates the production of NO_3^- by nitrification of NH_4^+ in the unsaturated zone and nil transport to the lower layers due to the low hydraulic conductivity of the sediments and/or the attenuation by denitrification.

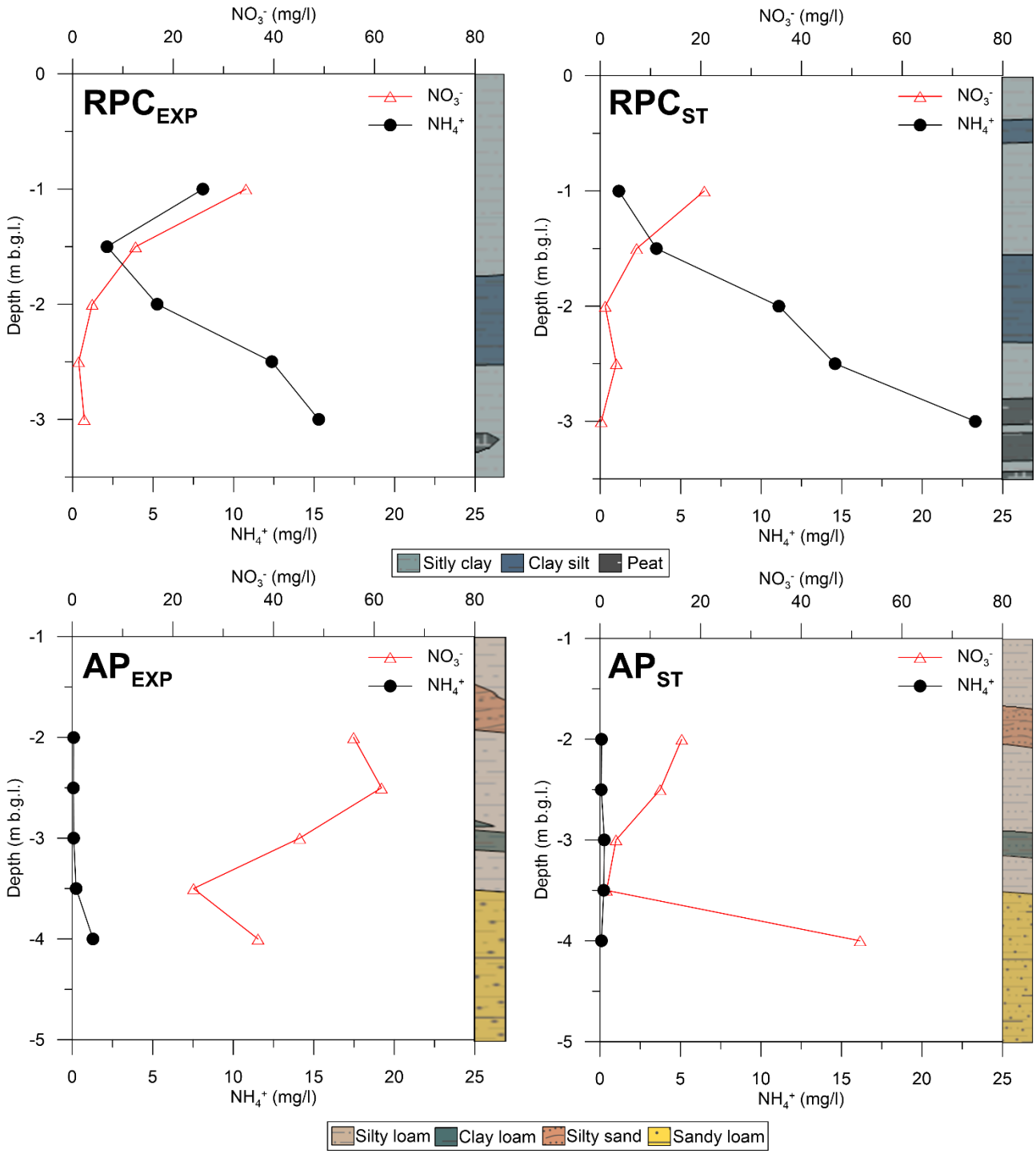

Figure 6. NO_3^- and NH_4^+ groundwater concentrations depth profiles in RCP and AP sites.

In AP, due to its mainly oxic conditions, NO_3^- is the main reactive N species, while NH_4^+ concentration is nil or very low. NO_3^- concentrations show values of 58.0 and 16.2 mg/L in the shallow MLS ports, a decrease with depth and show a reverse trend toward higher concentrations in the deep MLS ports, especially in AP_{ST}. The latest is most probably due to the horizontal transport

of NO_3^- from upgradient sources located in other agricultural fields. A small amount of NH_4^+ is also observed in the deep MLS ports, especially in AP_{EXP}, again probably due to upgradient sources. NO_3^- concentrations pattern in AP_{EXP} and AP_{ST} suggests NO_3^- attenuation by denitrification and the contribution of an additional source of reactive N located upgradient respect to the monitored agricultural field and transported along the groundwater regional head gradient. The elevated difference in NO_3^- concentrations between AP_{EXP} and AP_{ST}, highlights that local heterogeneities of hydraulic conductivity, infiltration rates and fertilizer concentrations are very pronounced in AP.

3.4.2 Isotope data on NH_4^+ and NO_3^-

Further insight about the sources and the fate of N species at the study site can be provided by the isotope data on NH_4^+ and NO_3^-. Concerning NH_4^+, a clear inverse trend between $\delta^{15}N\text{-}NH_4^+$ and NH_4^+ concentration is observed at both RCP_{ST} and RCP_{EXP} (Figure 7). $\delta^{15}N\text{-}NH_4^+$ data show values around +7 ‰ near the water table, reaching +3.5 ‰ within the peat lenses. These results agree with previous results obtained in this area (Caschetto et al., 2017), where the upper part of the aquifer was characterized by enriched $\delta^{15}N\text{-}NH_4^+$ values (from 4.4‰ up to 7.1‰) and the lower part of the aquifer was characterized by lower $\delta^{15}N\text{-}NH_4^+$ values (from 1‰ to 2.7‰). Furthermore, $\delta^{15}N\text{-}NH_4^+$ values of +2-3‰ are frequently associated with a natural organic N source (Kendall and Aravena, 2000), confirming that the source of the elevated NH_4^+ content in both RCP_{EXP} and RCP_{ST} profiles, at depth lower than -2 m b.g.l., is the mineralization of organic N-rich peat lenses, as originally proposed by Mastrocicco et al. (2013). Conversely, the higher than expected values of $\delta^{15}N\text{-}NH_4^+$ found in the upper portion of both RCP_{EXP} and RCP_{ST} profiles could be due to partial NH_4^+ nitrification from fertilizers. In fact, nitrification processes tend to enrich the remaining NH_4^+ pool respect to the original N fertilizers median value of 0.0‰ (Vitòria et al., 2004; Aravena and Mayer, 2010).

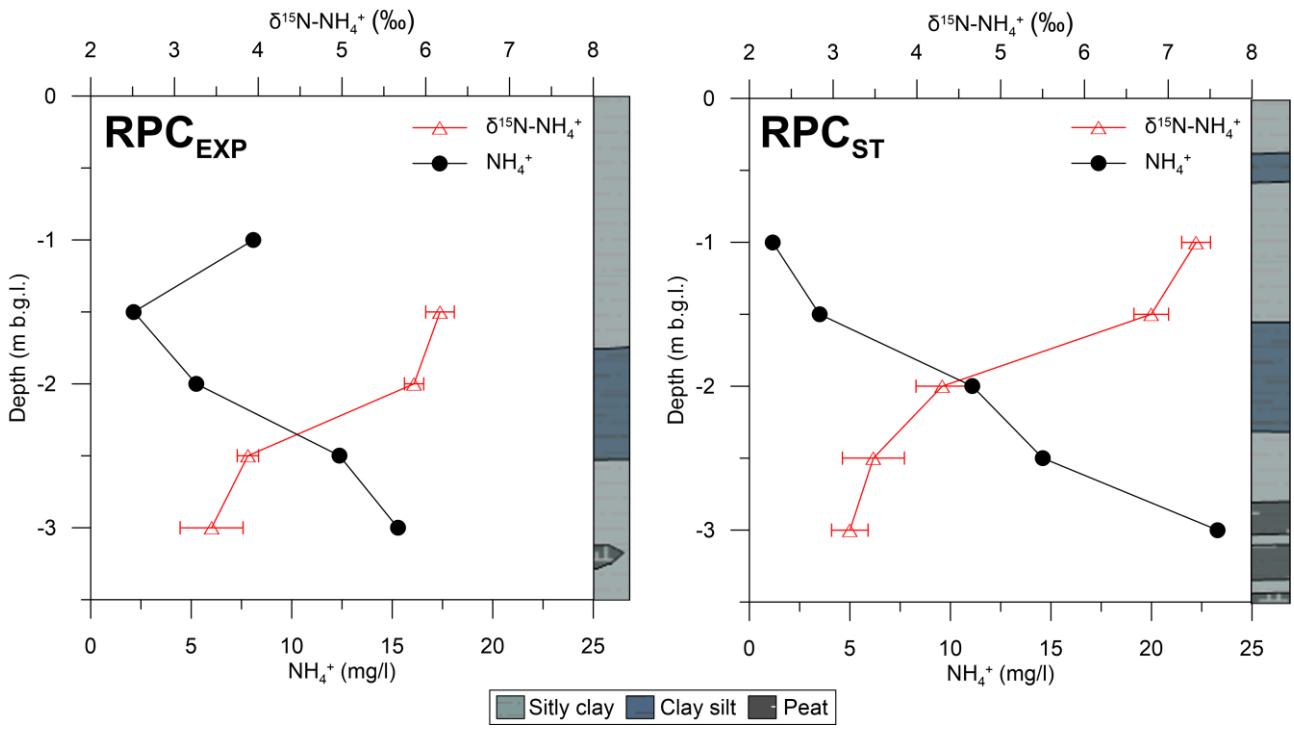

Figure 7. $\delta^{15}N\text{-}NH_4^+$ versus NH_4^+ groundwater concentrations depth profiles in RCP. Error bars for $\delta^{15}N\text{-}NH_4^+$ represent the standard deviation over three replicates.

Concerning NO_3^- pattern (Figure 8), the RCP_{EXP} profile shows $\delta^{15}N\text{-}NO_3^-$ values of +3.3‰ in the shallow port changing toward an enriched value of +13.6‰ and reversing to lower values of -1.8‰ and +5.6‰ in the deep port; while the RCP_{ST} profile shows an enriched $\delta^{15}N\text{-}NO_3$ value of +18.6‰ in the shallow port and a trend toward more depleted values of +0.2‰ and +6.1‰ with depth. Both profiles show a trend of decreasing NO_3^- concentration with depth but with slightly different concentrations in the shallow MLS ports, 34.5 mg/L in RCP_{ST} and 30.7 mg/L in RCP_{EXP}. Due to the reducing condition at RCP, the enriched $\delta^{15}N\text{-}NO_3^-$ values should be related to denitrification, as confirmed by the data in Figure 9 that show the relationship between $\delta^{18}O\text{-}NO_3^-$ vs $\delta^{15}N\text{-}NO_3^-$.

One set of data which included the enriched $\delta^{15}N\text{-}NO_3^-$ values at RCP shows the typical trend associated to denitrification. The most interesting data are the low NO_3^- concentration samples corresponding to the deepest MLS ports, that plot within the box of atmospheric deposition. This

implies that this part of the profile has been never affected by agriculture activities and preserve the isotope fingerprint of pre-agriculture activities.

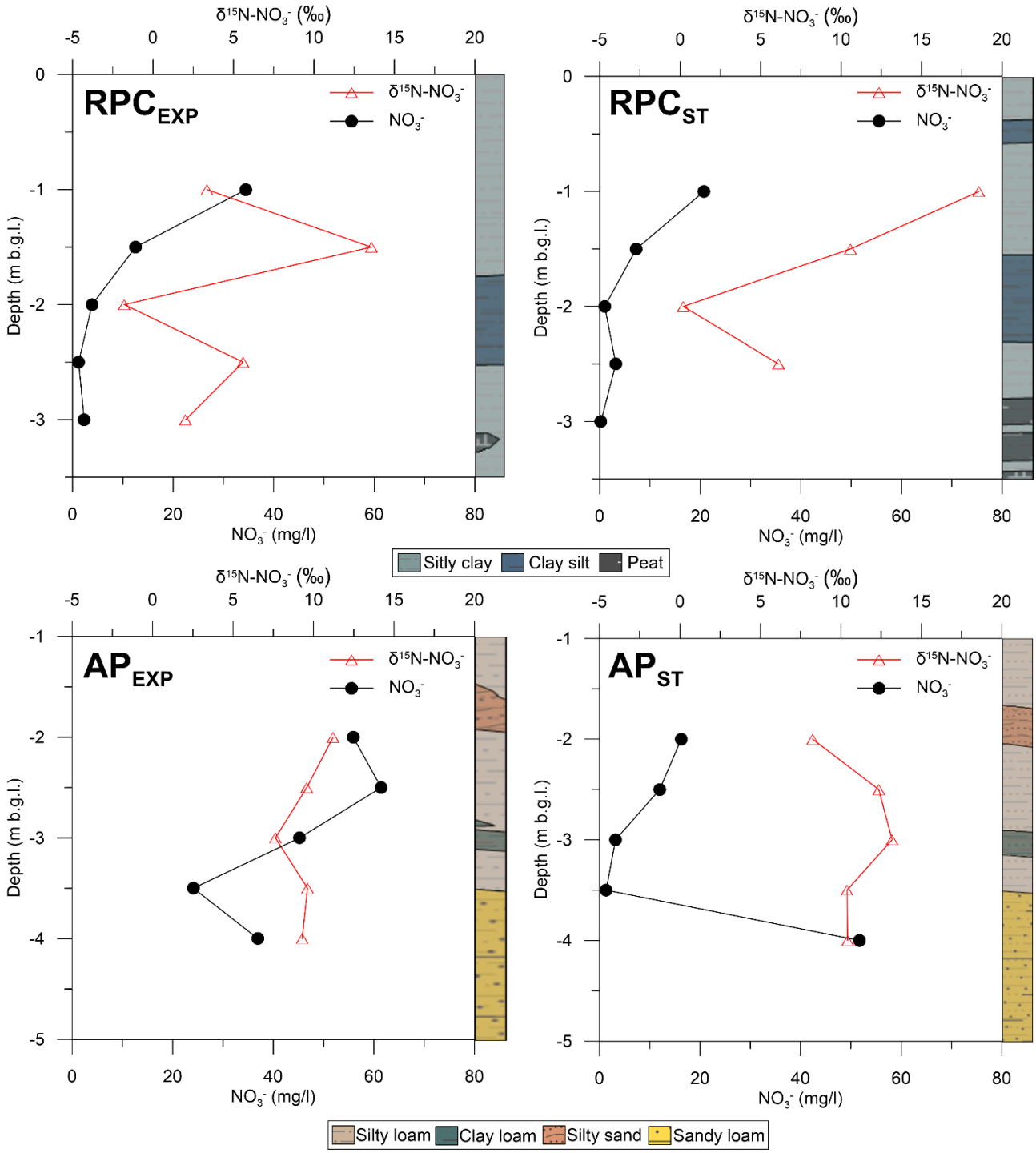

Figure 8. $\delta^{15}N\text{-}NO_3^-$ versus NO_3^- groundwater depth profiles in RCP and AP.

A contrasting pattern is observed at AP compared to RCP (Figure 8). No significant change is observed with depth at AP_{EXP}, that shows $\delta^{15}N\text{-}NO_3^-$ values of +11.2‰ in the shallow port and values between +9.6‰ and +7.6‰ in the deep port. In AP_{ST} the shallow port shows a values of +8.2‰ tending toward more enriched values of +12.2‰ and +13.1‰ and again towards lower values with depth (around +10‰). Both profiles show a decrease of NO_3^- concentration with depth, but in the deepest port of AP_{ST} NO_3^- concentration increased significantly in the sandy aquifer. Most of the data plot within the box of manure and septic system (Figure 9), however these values can be associated even to urea that have been affected by volatilization processes in the soil. The enriched $\delta^{15}N\text{-}NO_3^-$ values of +12.2 and +13.1 ‰ at AP_{ST} are also accompanied by enriched $\delta^{18}O\text{-}NO_3^-$ values, and plot in the trend associated to denitrification. This suggest that, despite of the oxic condition at the AP_{ST} site, denitrification probably associated to microsites under more reducing condition, is playing a role in nitrate cycling at the AP_{ST} site.

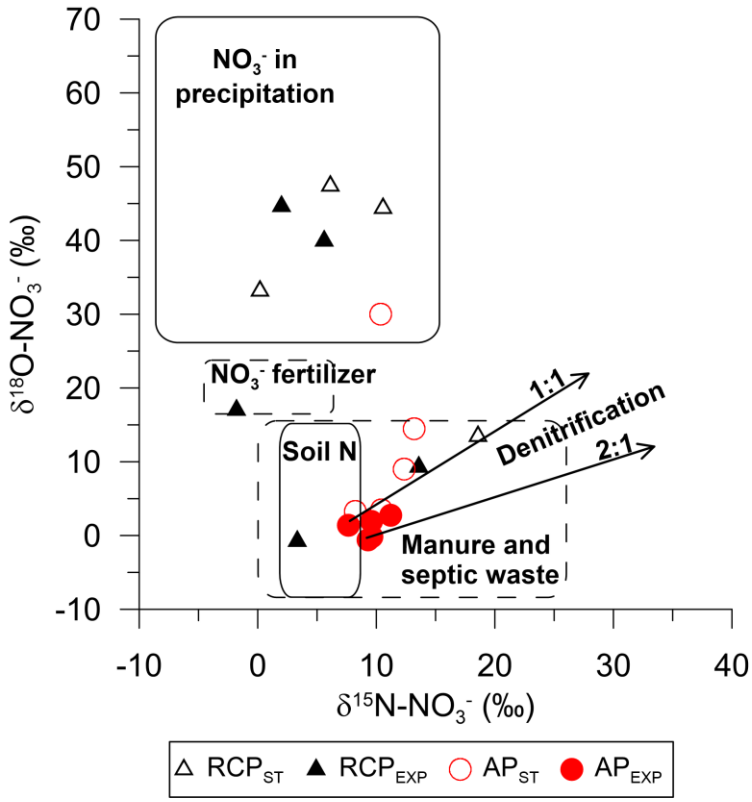

Figure 9. Scatter plot of $\delta^{15}N\text{-}NO_3^-$ versus $\delta^{18}O\text{-}NO_3^-$ in groundwater of RCP and AP sites. The typical isotopic compositions of different sources of NO_3^- are also shown (Kendall et al., 2007).

3.5. Sulphate isotope groundwater profiles

Since N and S cycles are controlled by redox conditions and sometimes are linked in groundwater, the stable isotope data on SO_4^{2-} will be analyzed in the context of redox conditions and possible link with the N cycle. The isotope data on SO_4^{2-} will be used to evaluate the sources and the processes that can affect SO_4^{2-} in groundwater. Figure 10 shows $\delta^{34}S\text{-}SO_4^{2-}$ profiles vs their respective SO_4^{2-} concentrations in RCP and AP; H_2S data, a by-product of SO_4^{2-} reduction, is also plotted for RCP. $\delta^{34}S\text{-}SO_4^{2-}$ values at RCP_{ST} are around 0.0‰ in the shallow MLS ports, tend toward enriched $\delta^{34}S\text{-}SO_4^{2-}$ values of +21.2‰ and +37.1‰ with depth, reversing to lower values in the deepest part of the profile. The shallow $\delta^{34}S\text{-}SO_4^{2-}$ values are typical of pyrite oxidation (Moncaster et al., 2000; Zhang et al., 2012), which could occur in the unsaturated zone. Besides, pyrite is common in these saline and organic rich environments (Colombani et al., 2015). The more enriched $\delta^{34}S\text{-}SO_4^{2-}$ values could be linked to SO_4^{2-} reduction (Böttcher et al., 2001), which is supported by the occurrence of high concentrations of H_2S (27.1 and 37.1 mg/L). The trend of decreasing SO_4^{2-} concentration in the interval of the enriched $\delta^{34}S\text{-}SO_4^{2-}$ values and the reducing conditions also support the occurrence of SO_4^{2-} reduction at RCP. A different pattern is observed in AP. First, a great variability in the shallow part of the aquifer is observed in the SO_4^{2-} concentration data, with values ranging from 326 to 411 mg/L in AP_{ST} and from 65 to 78 mg/L in AP_{EXP}. A trend toward higher concentration is observed with depth. A $\delta^{34}S\text{-}SO_4^{2-}$ value of around -2‰ in the whole profile is observed at AP_{ST} while a trend from values around -2‰ to -7‰ is observed at AP_{EXP} with depth. These $\delta^{34}S\text{-}SO_4^{2-}$ values are typical of SO_4^{2-} originating from the oxidation of sulphide minerals (Moncaster et al., 2000; Zhang et al., 2012). No evidence of SO_4^{2-} reduction is observed at AP since the redox conditions are not suitable for the occurrence of SO_4^{2-} reduction.

The evaluation of sources of SO_4^{2-} and processes that can affect SO_4^{2-} in groundwater can be further analysed using the relation between $\delta^{18}O$-SO_4^{2-} and $\delta^{34}S$-SO_4^{2-} (Figure 11). The data plotted in this figure tend to discard the proposition based only on the $\delta^{34}S$-SO_4^{2-} data that one of the sources of SO_4^{2-} could be pyrite oxidation. In fact, most data are within the box of the fertilizers, indicating that the source of SO_4^{2-} is more likely the use of fertilizers. SO_4^{2-} is present in the inorganic fertilizers used in the study area. However, $\delta^{18}O$-SO_4^{2} values in the range of 5 to 8 ‰ can be generated by oxidation of pyrite when oxygen plays a major role in the oxidation of pyrite (van Everdingen et al., 1985). Values greater than 8‰ could also be generated when water with more enriched $\delta^{18}O$-H_2O values than the current values measured at the study site has been involved in the oxidation of pyrite (Van Everdingen et al., 1985). Furthermore, the very high SO_4^{2-} concentrations reaching values as 1390 mg/L at the RCP site support the role of pyrite oxidation as one of the sources of SO_4^{2-} at the study site. The two apparent outliers observed in Figure 11, which correspond to the deeper samples at the RCP site (see supporting information), could be a reflection of a complex sulphur cycling in the older lagoons system at the study site. Then, the trend toward enriched $\delta^{18}O$-SO_4^{2-} and $\delta^{34}S$-SO_4^{2-} values support the interpretation, based on the $\delta^{34}S$-SO_4^{2-} and H_2S patterns, that SO_4^{2-} reduction is affecting the concentration of SO_4^{2-} at depth in RCP.

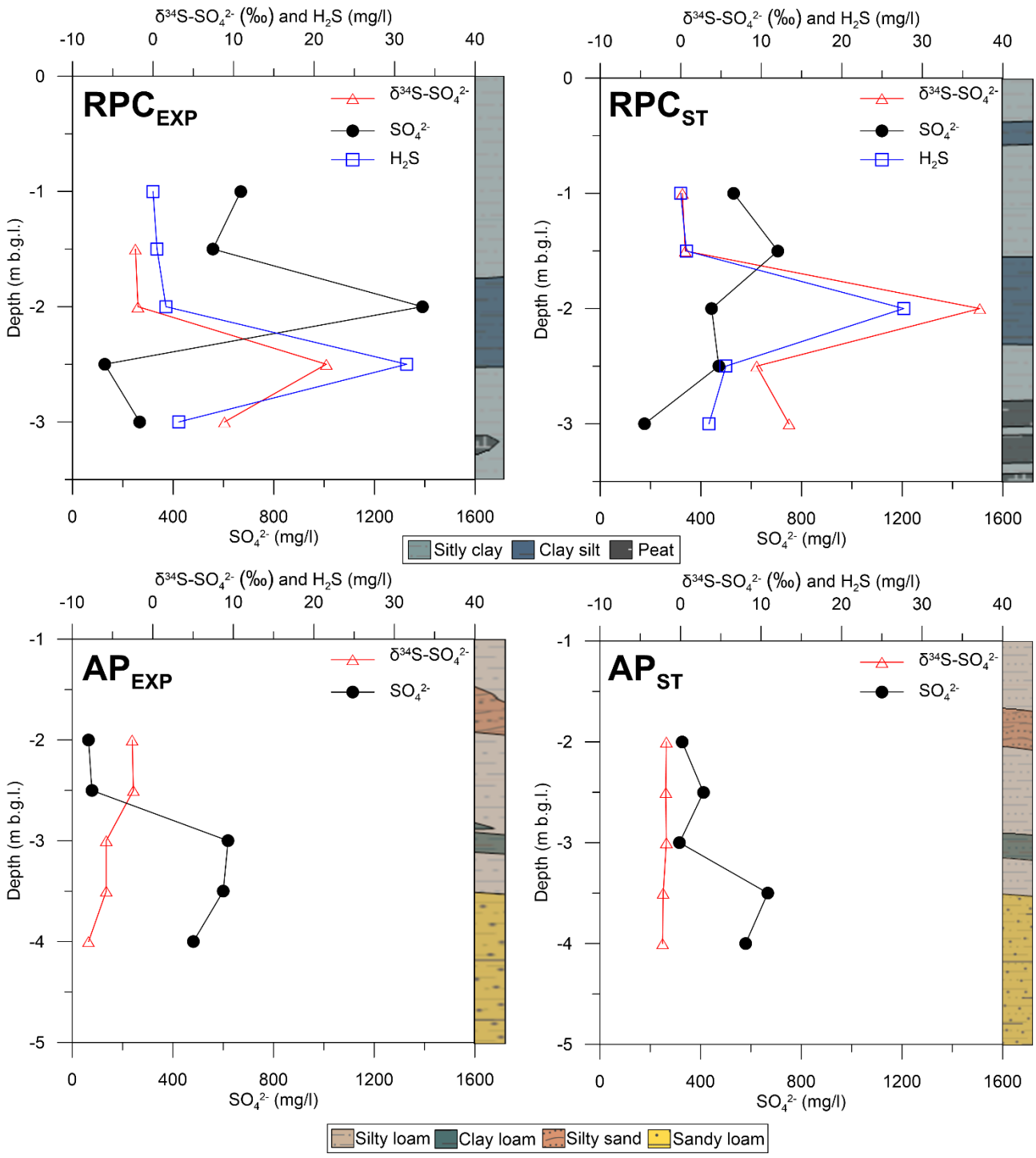

Figure 10. $\delta^{34}S\text{-}SO_4^{2-}$ versus SO_4^{2-} groundwater concentration depth profiles in RCP and AP. H_2S was also plotted for RCP. Note that in RCP_{EXP} the upper $\delta^{18}O\text{-}SO_4^{2-}$ value is not plotted since there was not enough sample to run the analyses.

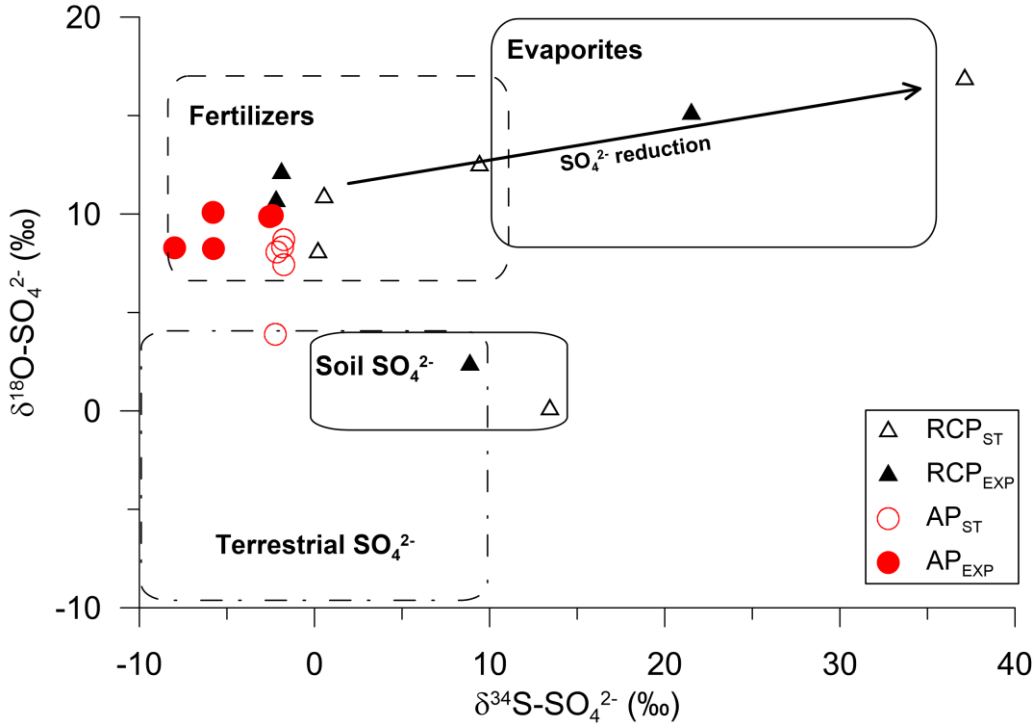

Figure 11. Scatter plot of $\delta^{34}S$-SO_4^{2-} versus $\delta^{18}O$-SO_4^{2-} in groundwater of RCP and AP sites. The typical isotopic compositions of different sources of SO_4^{2-} are also shown (Modified from Clark and Fritz, 1997 and Vitòria et al., 2004).

3.6. Organic and inorganic carbon isotopes groundwater profiles

The differences in redox conditions and reactivity between RCP and AP must be related to the nature of the sediments. RCP is characterized by the presence of organic rich sediments, which is reflected in the higher DOC content (from 13.2 to 54.55 mg-C/L) compared to the AP one (from 6.4 to 11.1 mg-C/L) (Table 2). The highly reducing condition of the groundwater at RCP is suitable not only for SO_4^{2-} reduction but also for methanogenesis. In fact, peaty lenses, like the ones found in RCP, usually trigger methanogenic conditions in shallow lowland aquifers (Caschetto et al., 2017; Schloemer et al., 2018) or in shallow upland aquifers (Clague et al., 2019). The increase of CH_4 and DIC concentrations with depth and the trend toward more enriched $\delta^{13}C$-DIC values with depth at RCP (Figure 12) are typical patterns associated to methanogenesis (Simpkins and Parkin, 1993; Aravena et al., 1995). The isotopic enrichment in the residual CO_2, that occurred during the

formation of CH_4 by CO_2 reduction, is very pronounced respect to the original CO_2 (Nowak et al., 2017). The enriched CO_2 is further recycled into the DIC pool through carbonate equilibrium reactions, causing the enrichment of δ^{13}C-DIC and an increase of DIC in groundwater (Aravena and Wassenaar, 1993; Aravena et al., 1995).

Table 2. DOC, DIC, and CH_4 concentrations values in groundwater samples for both RCP and AP.

Sample ID	Depth (m b.g.l.)	DOC (mg-C/L)	DIC (mg-C/L)	CH_4 (µg/L)	δ^{13}C-DIC (‰)
$RCP_{EXP}1$	-1.0	16.27	29.9	5.7	Not analysed
$RCP_{EXP}1.5$	-1.5	18.09	41.9	18.3	-10.9
$RCP_{EXP}2$	-2.0	33.99	44.3	214	-11.7
$RCP_{EXP}2.5$	-2.5	54.55	187	1254	-6.3
$RCP_{EXP}3$	-3.0	40.44	192	4252	-1.6
$RCP_{ST}1$	-1.0	13.21	36.0	12.8	-13.3
$RCP_{ST}1.5$	-1.5	22.29	48.1	52.3	-12.1
$RCP_{ST}2$	-2.0	23.12	84.0	64.5	-7.9
$RCP_{ST}2.5$	-2.5	37.40	72.2	3633	0.9
$RCP_{ST}3$	-3.0	36.36	198	9394	2.1
$AP_{ST}2$	-2.0	11.08	53.9	2.8	-7.6
$AP_{ST}2.5$	-2.5	7.34	60.2	2.7	-6.8
$AP_{ST}3$	-3.0	6.90	55.1	2.9	-8.4
$AP_{ST}3.5$	-3.5	10.89	72.0	2.7	-8.4
$AP_{ST}4$	-4.0	8.40	36.0	49.4	-9.9
$AP_{EXP}2$	-2.0	8.35	59.1	5.9	-8.7
$AP_{EXP}2.5$	-2.5	7.45	56.1	5.1	-10.2
$AP_{EXP}3$	-3.0	6.84	60.0	3.4	-9.4
$AP_{EXP}3.5$	-3.5	6.40	53.1	25.9	-9.2
$AP_{EXP}4$	-4.0	7.81	50.0	108	-10.4

Concerning the AP site, very low CH_4 is observed at this site excepting in the deeper sandy aquifer probably associated to an upgradient source. No appreciable changes are observed in the DIC and δ^{13}C-DIC values with depth (Figure 12, lower plots). The C isotope and concentration patterns have shown, beside SO_4^{2-} reduction as inferred for the SO_4^{2-} isotope data, that methanogenesis is also occurring in groundwater at RCP.

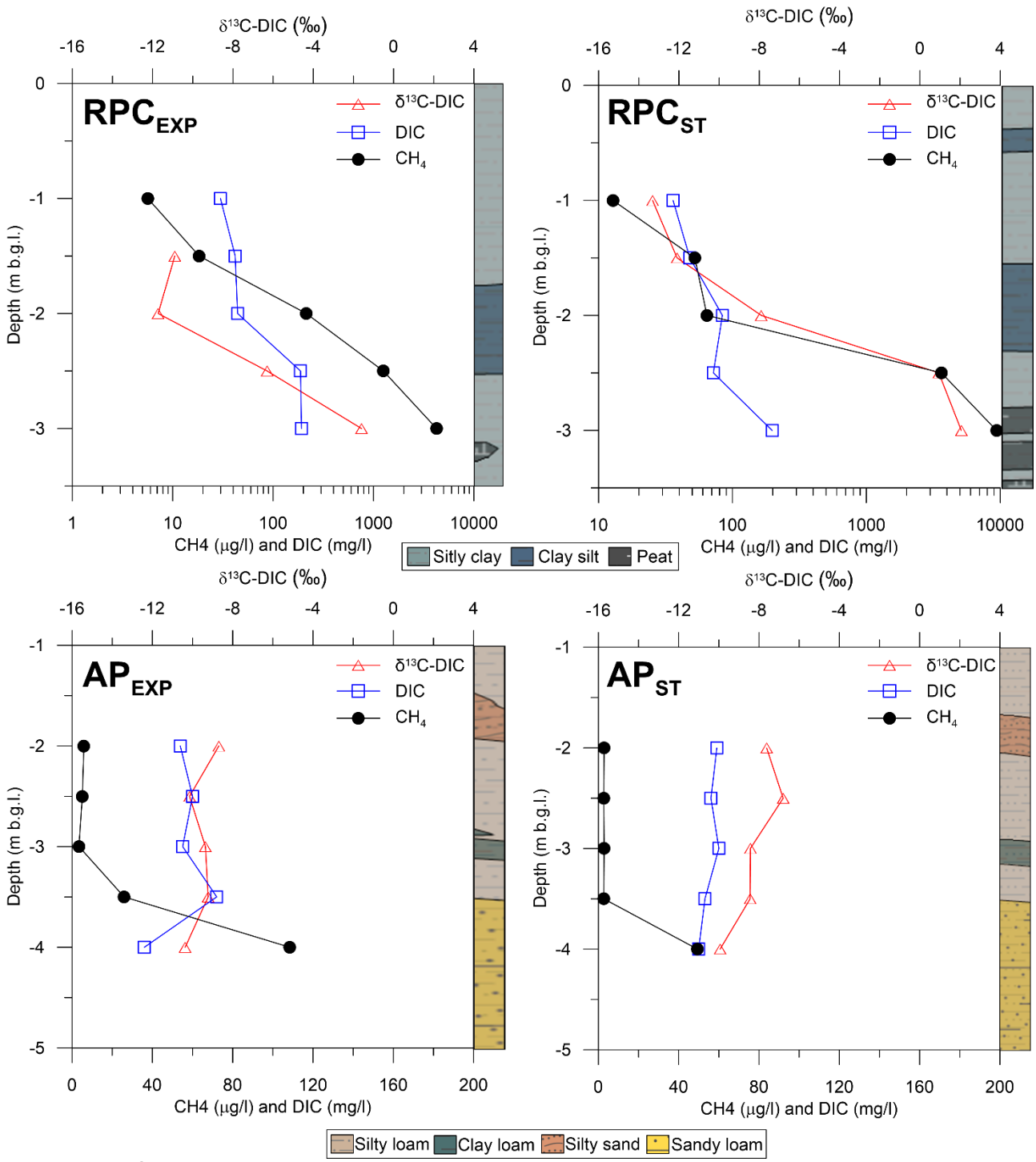

Figure 12. δ^{13}C-DIC versus DIC and CH_4 groundwater concentration depth profiles in RCP and AP sites. Note that in RCPEXP the upper δ^{13}C-DIC value is not plotted since there was not enough sample to run the analyses.

4. Conclusions

This study has shown a clear distinction between different sources of reactive N species present in intensely cultivated freshwater paleo-river environments (AP) and reclaimed brackish swamp environments (RCP) of the Po Delta, from synthetic fertilizers to sedimentary N pool and atmospheric input. The presence of sedimentary N and atmospheric N input were well documented at the RCP site, which is characterized by rich organic sediments deposited in a marshy environment. Denitrification was documented to occur in the RCP and AP_{ST} sites. The SO_4^{2-} isotope data shown that pyrite and fertilizers are the main sources of the large amount of SO_4^{2-} found in groundwater in both sites.. The occurrence of SO_4^{2-} reduction and methanogenesis were also documented at RCP, by the isotope data on SO_4^{2-} and DIC, respectively. The presence of relative high amount of CH_4 and H_2S at RCP supports the interpretation of the isotope data. Conversely, at AP no appreciable concentrations of H_2S and CH_4 were recorded, confirming the prevailing oxic conditions of this freshwater environment.

This study was part of a controlled agriculture experiment aiming to evaluate the effect that a change in the agriculture practices (from classical fertilization and tillage techniques to compost and no-tillage) may have in groundwater quality. However, the Br^- tracer test results show that the chemical and isotopic variability found in this study cannot be related to the actual agricultural practices but are instead related to historical practices, when the same fertilizers amount and ploughing techniques were employed in every plot at both sites. Thus, the different geochemical patterns observed between the two sites, and even within each site at different plots, could be related only to the nature of the sediments and the source of irrigation water. For instance, at RCP high SOM and low hydraulic conductivity created different redox conditions with respect to the AP site. Furthermore, the sources of water, which include local precipitation and irrigation water associated to the Po river, could be also an element to be considered to explain the different geochemical responses at the study sites.

A key outcome of this study is that high resolution monitoring and tracer tests in the unsaturated zone are key elements that must be implemented to evaluate the response in groundwater quality to changes in agriculture practices aiming to reduce the amount of N reaching shallow groundwaters.

Acknowledgments

This work was financially supported by the Emilia-Romagna Region within the Rural Development Programme (PSR) 2014-2020 and within the POR FESR 2007-2013 Programme for the development of the regional High Technology Network.

References

Aravena, R., Mayer, B., 2010. Isotopes and Processes in the Nitrogen and Sulfur Cycles. In Environmental Isotopes in Biodegradation and Bioremediation; CRC Press/Lewis: Boca Raton, FL, USA, 203-246. ISBN: 9781566706612.

Aravena, R., Robertson, W.D., 1998. Use of Multiple Isotope Tracers to Evaluate Denitrification in Ground Water: Study of Nitrate from a Large-Flux Septic System Plume. Groundwater 36, 975-982. Doi: 10.1111/j.1745-6584.1998.tb02104.x.

Aravena, R., Wassenaar, L.I., 1993. Dissolved organic carbon and methane in a regional confined aquifer, southern Ontario, Canada: Carbon isotope evidence for associated subsurface sources. Appl. Geochem. 8(5), 483-493. Doi: 10.1016/0883-2927(93)90077-T.

Aravena, R., Wassenaar, L.I., Plummer, L.N., 1995. Estimating ^{14}C groundwater ages in a methanogenic aquifer. Water Resour. Res. 31(9), 2307-2317. Doi: 10.1029/95WR01271.

Biddau, R., Cidu, R., Da Pelo, S., Carletti, A., Ghiglieri, G., Pittalis, D., 2019. Source and fate of nitrate in contaminated groundwater systems: assessing spatial and temporal variations by hydrogeochemistry and multiple stable isotope tools. Sci. Tot. Environ. 647, 1121-1136. Doi: 10.1016/j.scitotenv.2018.08.007

Böhlke, J.K., 2002. Groundwater recharge and agricultural contamination. Hydrogeol. J. 10, 153-179. Doi: 10.1007/s10040-001-0183-3.

Böhlke, J.K., Denver, J.M., 1995. Combined use of groundwater dating, chemical, and isotopic analyses to resolve the history and fate of nitrate contamination in two agricultural watersheds, Atlantic coastal plain, Maryland. Water Resour. Res. 31(9), 2319-2339. Doi: 10.1029/95WR01584.

Böttcher, M.E., Thamdrup, B., Vennemann, T.W., 2001. Oxygen and sulphur isotope fractionation during anaerobic bacterial disproportionation of elemental sulphur. Geochim. Cosmochim. Acta 65 (10), 1601–1609. Doi: 10.1016/S0016-7037(00)00628-1.

Bouwer H., Rice R.C., 1976. A slug test for determining hydraulic conductivity of unconfined aquifers with completely or partially penetrating wells. Water Resour. Res. 12(3), 423–428. Doi: 10.1029/WR012i003p00423.

Caschetto, M., Colombani, N., Mastrocicco, M., Petitta, M., Aravena, R., 2017. Nitrogen and sulphur cycling in the saline coastal aquifer of Ferrara, Italy. A multi-isotope approach. Appl. Geochem. 76, 88-98. Doi: 10.1016/j.apgeochem.2016.11.014.

Castaldelli, G., Soana, E., Racchetti, E., Pierobon, E., Mastrocicco, M., Tesini, E., Fano, E.A., Bartoli, M., 2013. Nitrogen budget in a lowland coastal area within the Po river basin (Northern

Italy): multiple evidences of equilibrium between sources and internal sinks. Environ. Manage. 52(3), 567-580. Doi: 10.1007/s00267-013-0052-6.

Clague, J. C., Stenger, R., Morgenstern, U., 2019. The influence of unsaturated zone drainage status on denitrification and the redox succession in shallow groundwater. Sci. Tot. Environ. 600, 1232-1244. Doi: 10.1016/j.scitotenv.2018.12.383.

Clark, I.D., Fritz, P., 1997. Environmental Isotopes in Hydrogeology. Lewis, New York ,328 pp.

Colombani, N., Di Giuseppe, D., Faccini, B., Ferretti, G., Mastrocicco, M., Coltorti, M., 2016. Inferring the interconnections between surface water bodies, tile-drains and an unconfined aquifer–aquitard system: a case study. J. Hydrol. 537, 86-95. Doi: 10.1016/j.jhydrol.2016.03.046.

Colombani, N., Mastrocicco, M., Dinelli, E., 2015. Trace elements mobility in a saline coastal aquifer of the Po river lowland (Italy). J. Geochem. Explor. 159, 317-328. Doi: 10.1016/j.gexplo.2015.10.009-

Criss, R.E., Davisson, M.L., 1996. Isotopic imaging of surface water/groundwater interactions, Sacramento Valley, California. J. Hydrol. 178(1-4), 205-222. Doi: 10.1016/0022-1694(96)83733-4.

Curzi, P.V., Dinelli, E., Lucchi, M.R., Vaiani, S.C, 2006. Palaeoenvironmental control on sediment composition and provenance in the late Quaternary deltaic successions: A case study from the Po delta area (Northern Italy). Geolog. J. 41(5), 591-612. Doi: 10.1002/gj.1060.

Fernández, E., Grilli, A., Alvarez, D., Aravena, R., 2017. Evaluation of nitrate levels in groundwater under agricultural fields in two pilot areas in central Chile: A hydrogeological and geochemical approach. Hydrol. Proc. 31(6), 1206-1224. Doi: 10.1002/hyp.11103.

Giustini, F., Brilli, M., Patera, A., 2016. Mapping oxygen stable isotopes of precipitation in Italy. J. Hydrol. Region. Stud. 8, 162-181. Doi: 10.1016/j.ejrh.2016.04.001.

Green, C.T., Liao, L., Nolan, B.T., Juckem, P.F., Shope, C.L., Tesoriero, A.J., Jurgens, B.C., 2018. Regional variability of nitrate fluxes in the unsaturated zone and groundwater, Wisconsin, USA. Water Resour. Rese. 54(1), 301-322. Doi: 10.1002/2017WR022012.

Greggio, N., Giambastiani, B.M.S., Campo, B., Dinelli, E., Amorosi, A., 2018. Sediment composition, provenance, and Holocene paleoenvironmental evolution of the Southern Po River coastal plain (Italy). Geol. J. 53(3), 914-928. Doi: 10.1002/gj.2934.

Griffioen, J., Vermooten, S., Janssen, G., 2013. Geochemical and palaeohydrological controls on the composition of shallow groundwater in the Netherlands. Appl. Geochem. 39, 129-149. Doi: 10.1016/j.apgeochem.2013.10.005.

Horita, J., K. Rozanski, Cohen, S., 2008. Isotope effects in the evaporation of water: A status report of the Craig-Gordon model. Isot. Environ. Health Stud. 44(1), 23–49. Doi:10.1080/10256010801887174.

Hosono, T., Tokunaga, T., Kagabu, M., Nakata, H., Orishikida, T., Lin, I. T., Shimada, J., 2013. The use of $\delta^{15}N$ and $\delta^{18}O$ tracers with an understanding of groundwater flow dynamics for

evaluating the origins and attenuation mechanisms of nitrate pollution. Water Res. 47(8), 2661-2675. Doi: 10.1016/j.watres.2013.02.020.

Kaown, D., Koh, D.-C., Mayer, B., Lee, K.-K., 2009. Identification of nitrate and sulphate sources in groundwater using dual stable isotope approaches for an agricultural area with different land use (Chuncheon, mid-eastern Korea). Agric. Ecosyst. Environ. 132, 223-231. Doi: 10.1016/j.agee.2009.04.004.

Kendall, C., Aravena, R., 2000. Nitrate isotopes in groundwater systems. In: Cook, P.G., Hercseg, A.L. (Eds.), Environmental Tracers in Subsurface Hydrology. Kluwer Academic Press, New York, pp. 261–297.

Kendall, C., Elliott, E.M., Wankel, S.D., 2007. Tracing Anthropogenic Inputs of Nitrogen to Ecosystems. In Stable Isotopes in Ecology and Environmental Science, 2nd Ed. Lajtha, K., Michener, R.H., Eds. Blackwell Publishing, London.

Martinelli, G., Dadomo, A., De Luca, D. A., Mazzola, M., Lasagna, M., Pennisi, M., Pilla, G., Sacchi E., Saccon, P., 2018. Nitrate sources, accumulation and reduction in groundwater from Northern Italy: insights provided by a nitrate and boron isotopic database. Appl. Geochem. 91, 23-35. Doi: 10.1016/j.apgeochem.2018.01.011.

Mastrocicco, M., Colombani, N., Palpacelli, S., Castaldelli, G., 2011. Large tank experiment on nitrate fate and transport: the role of hydraulic conductivity distribution. Environ. Earth Scie. 63(5), 903-914. Doi: 10.1007/s12665-010-0759-0.

Mastrocicco, M., Di Giuseppe, D., Vincenzi, F., Colombani, N., Castaldelli, G., 2017. Chlorate origin and fate in shallow groundwater below agricultural landscapes. Environ. Pollut. 231, 1453-1462. Doi: 10.1016/j.envpol.2017.09.007.

Mastrocicco, M., Giambastiani, B. M. S., Colombani, N., 2013. Ammonium occurrence in a salinized lowland coastal aquifer (Ferrara, Italy). Hydrol. Process. 27(24), 3495-3501. Doi: 10.1002/hyp.9467.

Mayer, B., Krouse, H.R., 2004. Procedures for sulphur isotope abundance studies. Handb. Stable Isotope Anal. Tech. 538–596.

Moncaster, S.J., Bottrell, S H., Tellam, J.H., Lloyd, J.W., Konhauser, K.O., 2000. Migration and attenuation of agrochemical pollutants: insights from isotopic analysis of groundwater sulphate. J. Cont. Hydrol. 43(2), 147-163. Doi: 10.1016/S0169-7722(99)00104-7.

Nowak, M., Schwab, V.F., Lazar, C S., Behrendt, T., Kohlhepp, B., Totsche, K.U., Kirsten Küsel, K., Trumbore, S.E., 2017. Carbon isotopes of dissolved inorganic carbon reflect utilization of different carbon sources by microbial communities in two limestone aquifer assemblages. Hydrol. Earth Syst. Sci. 21(9), 4283-4300. Doi:10.5194/hess-21-4283-2017.

Oenema, O., van Liere, L., Schoumans, O., 2005. Effects of lowering nitrogen and phosphorus surpluses in agriculture on the quality of groundwater and surface water in the Netherlands. J. Hydrol. 304(1-4), 289-301. Doi: 10.1016/j.jhydrol.2004.07.044.

Paradis, D., Ballard, J.M., Lefebvre, R., Savard, M.M., 2018. Multi-scale nitrate transport in a sandstone aquifer system under intensive agriculture. Hydrogeol. J. 26(2), 511-531. Doi: 10.1007/s10040-017-1668-z.

Pauwels, H., Ayraud-Vergnaud, V., Aquilina, L., Molénat, J., 2010. The fate of nitrogen and sulfur in hard-rock aquifers as shown by sulphate-isotope tracing. Appl. Geochem. 25(1), 105-115. Doi: 10.1016/j.apgeochem.2009.11.001.

Puig, R., Soler, A., Widory, D., Mas-Pla, J., Domènech, C., Otero, N., 2017. Characterizing sources and natural attenuation of nitrate contamination in the Baix Ter aquifer system (NE Spain) using a multi-isotope approach. Sci. Tot. Environ. 580, 518-532. Doi: 10.1016/j.scitotenv.2016.11.206.

Rivett, M.O., Buss, S.R., Morgan, P., Smith, J.W., Bemment, C.D., 2008. Nitrate attenuation in groundwater: a review of biogeochemical controlling processes. Water Res. 42(16), 4215-4232. Doi: 10.1016/j.watres.2008.07.020.

Ryabenko, E., Altabet, M.A., Wallace, D.W., 2009. Effect of chloride on the chemical conversion of nitrate to nitrous oxide for $\delta^{15}N$ analysis. Limnol. Oceanogr. 7, 545–552. Doi: 10.4319/lom.2009.7.545.

Schloemer, S., Oest, J., Illing, C. J., Elbracht, J., Blumenberg, M., 2018. Spatial distribution and temporal variation of methane, ethane and propane background levels in shallow aquifers–A case study from Lower Saxony (Germany). J. Hydrol. Regional Studies, 19, 57-79. Doi: 10.1016/j.ejrh.2018.07.002.

Simpkins, W.W., Parkin, T.B., 1993. Hydrogeology and redox geochemistry of CH_4 in a late Wisconsinan till and loess sequence in central Iowa. Water Resour. Res. 29(11), 3643-3657. Doi: 10.1029/93WR01687.

Taylor, P.G., Townsend, A.R., 2010. Stoichiometric control of organic carbon–nitrate relationships from soils to the sea. Nature 464(7292), 1178-1181. Doi: 10.1038/nature08985.

van Everdingen, R.O., Asif Shakur, M., Michel, F.A., 1985. Oxygen- and sulfur-isotope geochemistry of acidic groundwater discharge in British Columbia, Yukon, and District of Mackenzie, Canada. Canad. J. Earth Sci. 22, 1689-1695. Doi:10.1139/e85-177.

Vitòria, L., Otero, N., Soler, A., Canals, À., 2004. Fertilizer characterization: isotopic data (N, S, O, C, and Sr). Environ. Sci. Technol. 38(12), 3254-3262. Doi: 10.1021/es0348187.

Wang, X. S., Jiao, J. J., Wang, Y., Cherry, J. A., Kuang, X., Liu, K., Lee, C., Gong, Z., 2013. Accumulation and transport of ammonium in aquitards in the Pearl River Delta (China) in the last 10,000 years: conceptual and numerical models. Hydrogeol. J. 21(5), 961-976. Doi: 10.1007/s10040-013-0976-1.

Wu, J., Sun, Z., 2016. Evaluation of shallow groundwater contamination and associated human health risk in an alluvial plain impacted by agricultural and industrial activities, mid-west China. Expo. Health 8(3), 311-329. Doi: 10.1007/s12403-015-0170-x.

Yan, S., Liu, Y., Liu, C., Shi, L., Shang, J., Shan, H., Zachara, J., Fredrickson, J., Kennedy, D., Resch, C.T., Thompson, C., Fansler, S., 2016. Nitrate bioreduction in redox-variable low permeability sediments. Sci. Tot. Environ. 539, 185-195. Doi: 10.1016/j.scitotenv.2015.08.122.

Zhang, Y.C., Prommer, H., Broers, H.P., Slomp, C.P., Greskowiak, J., Van Der Grift, B., Van Cappellen, P., 2013. Model-based integration and analysis of biogeochemical and isotopic dynamics in a nitrate-polluted pyritic aquifer. Environ. Sci. Technol. 47(18), 10415-10422. Doi: 10.1021/es4023909.

Zhang, Y.C., Slomp, C.P., Broers, H.P., Bostick, B., Passier, H.F., Böttcher, M.E., Omoregie E.O., Lloyd, J.R., Polya, D.A., Van Cappellen, P., 2012. Isotopic and microbiological signatures of pyrite-driven denitrification in a sandy aquifer. Chem. Geol. 300, 123-132. Doi: 10.1016/j.chemgeo.2012.01.024